Microchim Acta (2014) 181:949–956
DOI 10.1007/s00604-014-1183-z

ORIGINAL PAPER

A magnetic metal-organic framework as a new sorbent for solid-phase extraction of copper(II), and its determination by electrothermal AAS

Yang Wang · Jing Xie · Yichun Wu · Xiaoya Hu

Received: 8 September 2013 / Accepted: 26 January 2014 / Published online: 14 February 2014

Abstract We report on the synthesis of Fe_3O_4-functionalized metal-organic framework (m-MOF) composite from Zn(II) and 2-aminoterephthalic acid by a hydrothermal reaction. The magnetic composite is iso-reticular and was characterized by FTIR, X-ray diffraction, SEM, magnetization, and TGA. The m-MOF was then applied as a sorbent for the solid-phase extraction of trace levels of copper ions with subsequent quantification by electrothermal AAS. The amount of sorbent applied, the pH of the sample solution, extraction time, eluent concentration and volume, and desorption time were optimized. Under the optimum conditions, the enrichment factor is 50, and the sorption capacity of the material is 2.4 mg g^{-1}. The calibration plot is linear over the 0.1 to 10 μg L^{-1} Cu(II) concentration range, the relative standard deviation is 0.4 % at a level of 0.1 μg L^{-1} (for n=10), and the detection limit is as low as 73 ng L^{-1}. We consider this magnetic MOF composite to be a promising and highly efficient material for the preconcentration of metal ions.

Keywords Fe_3O_4 · IRMOF-3 · Electrothermal atomic absorption spectrometry · Copper

Introduction

Solid-phase extraction (SPE) is becoming increasingly used as a sample pretreatment technology in the laboratory because of its merits of simplicity, low cost, low consumption of organic solvents, and high enrichment factor [1]. Recently, a new procedure for SPE, magnetic solid-phase extraction (MSPE), has been developed [2]. It is based on the use of magnetic or magnetically modified sorbents. In the MSPE method, the magnetic sorbents with adsorbed analytes can be easily separated from the sample matrix by the use of an external permanent magnet. Consequently, MSPE makes separation faster and easier, and avoids the time-consuming column passing or filtration operations encountered in SPE.

To date, many types of magnetic materials have been used for MSPE, such as magnetic carbon nanotubes [3], magnetic graphene nanocomposite [4], magnetic C18 microspheres [5], alumina-coated magnetite nanomaterials [6], and silica-coated magnetite microspheres [7]. Nevertheless, an important core task for enabling the widespread use of the MSPE method is to develop novel magnetic sorbents. For example, Zhou et al. reported the exploration of coordination polymers as a sorbent for SPE for the first time [8]. Cui et al. demonstrated the first example of the utilization of MOFs for SPME [9]. Yu et al. used a covalent bonding approach to fabricate a robust metal-organic framework ZIF-90 coating for SPME [10].

Metal-organic frameworks (MOFs), built up from organic linkers and inorganic connectors, have emerged as a new class of structured microporous material. The application of MOFs in hydrogen storage, gas sorption and separation, catalysis, and drug delivery has been reported. Recently, MOFs have been employed as stationary phases for gas chromatography [11–14], high-performance liquid chromatography [15–17] and capillary electrokinetic chromatography [18] to separate and determine organic pollutants in environmental matrices, such as polycyclic aromatic hydrocarbons (PAHs) [19], benzene homologues [20, 21], alkane isomers [22, 23] and organic phosphonates [24]. Furthermore, MOFs exhibit high activity and selectivity in adsorption, and there is growing interest particularly in the use of MOFs for SPME to adsorb and separate metal ions. Bagheri et al. utilized (Fe_3O_4-Pyridine)/

Electronic supplementary material The online version of this article (doi:10.1007/s00604-014-1183-z) contains supplementary material, which is available to authorized users.

Y. Wang (✉) · J. Xie · Y. Wu · X. Hu (✉)
College of Chemistry and Chemical Engineering, Yangzhou University, Yangzhou 225002, China
e-mail: wangyzu@126.com
e-mail: xyhu@yzu.edu.cn

$Cu_3(BTC)_2$ for preconcentration of Pd(II) for detection by flame atomic absorption spectrometry [25]. Sohrabi et al. utilized magnetic MOF Fe_3O_4-pyridine nanocomposite as an adsorbent for separation and preconcentration of Cd(II) and Pb(II) ions [26]. Taghizadeh et al. prepared a novel magnetic MOF DHz nanocomposite for the preconcentration of heavy metal ions [27].

Yaghi's group have developed iso-reticular MOFs (IRMOFs) to demonstrate that the three-dimensional porous system can be functionalized with the groups –Br, $–NH_2$, $–OC_3H_7$, $–OC_5H_{11}$, $–C_2H_4$, and $–C_4H_4$ and its pore size can be expanded with the long molecular struts biphenyl, tetrahydropyrene, pyrene, and terphenyl [28]. Among IRMOFs, IRMOF-3 ($Zn_4O(BDC\text{-}NH_2)_3$) is of particular interest due to the presence of the free amine functionality in the linkers [29]. The amino group on the 1,4-benzenedicarboxylate allows chemical reactions to occur in the pores of MOF materials. However, the application of IRMOF-3 to the analysis of heavy metals has not been reported before.

In this work, an MSPE method with Fe_3O_4/IRMOF-3 particles as sorbent for the separation and preconcentration of copper was established before sensitive determination by electrothermal atomic absorption spectrometry (ETAAS). It has been recognized that copper is an indispensable micronutrient in human health, which has important effects on the blood, central nervous system and immune system. High intake of copper, however, can be fatal: a concentration of 1.3 ppm can cause immediate effects on the human body in the form of vomiting, diarrhea, and nausea [30]. Consequently, copper was chosen as a model analysis material. To the best of our knowledge, this may be the first report on the determination of copper by using MSPE with Fe_3O_4/IRMOF-3 as sorbent. All the important parameters of the method were studied and optimized to enhance its effectiveness. The method was applied in the analysis of environmental water samples and certified reference materials.

Experimental

Apparatus

A Zeenit700 atomic absorption spectrometer (Germany, http://www.analytik-jena.com) was employed for the determination of copper. A copper hollow cathode lamp was used as the radiation source at 324.8 nm. Measurements were carried out in the integrated absorbance (peak area) mode at 6 mA, using a spectral bandwidth of 0.2 nm. A Tensor 27 spectrometer (Germany, http://www.bruker-axs.com) was used to obtain Fourier transform infrared (FTIR) spectra. X-ray diffraction (XRD) patterns were recorded on a D8 Advance X-ray diffractometer (Germany, http://www.bruker-axs.com) at room temperature. Field emission scanning electron micrographs (SEM) were obtained with a Hitachi S-4800 microscope (Japan, http://www.hitachi.com) at an acceleration voltage of 15 kV. The magnetic property was analyzed by using a vibrating sample magnetometer (America, http://www.ade.com). Thermogravimetric analysis (TGA) was performed by means of a Pyris 1 TGA (America, http://www.perkinelmer.com), under N_2 at a scan rate of 10 °C min^{-1}. A permanent magnet was used to enable the isolation of the analytes from the complicated matrix.

Reagents and materials

The stock standard solution containing 1,000 mg L^{-1} of Cu^{2+} was prepared by dissolving 1.9024 g $Cu(NO_3)_2 \cdot 3H_2O$ in 500 mL 0.5 mol L^{-1} nitric acid and working standard solutions were obtained by appropriate stepwise dilution of the stock standard solution. 2-Aminoterephthalic acid (R_3-BDC, America, http://www.sigma-aldrich.com); zinc nitrate, ferrous chloride, ferric chloride, ethanol, and dimethylformamide (DMF) were at least of analytical reagent grade and obtained from Sinopharm Chemical Reagent Co., Ltd (Shanghai, China, http://www.reagent168.cn) unless otherwise stated. Double de-ionized water (18 MΩ cm) was used throughout the experiments. The reference materials, which were stream sediment (GBW07303a) and soil (GBW07405), were purchased from BHH Biotechnology Co., Ltd (Beijing, China, http://www.gbw114.org). All containers were treated with 10 % HNO_3 for at least 24 h, rinsed with de-ionized water, and dried at room temperature before usage.

Preparation of IRMOF-3

The fabrication process was established using an established procedure with minor modifications [31]: Briefly, 0.5950 g (2 mmol) $Zn(NO_3)_2 \cdot 6H_2O$ in 5 mL DMF (solution A) and 0.0906 g (0.5 mmol) 2-aminoterephthalic acid in 5 mL DMF (solution B) were prepared. Solution A was then poured into solution B and mixed in a vial under ultrasound for 5 min. The mixed solution was poured into a 20 mL Teflon liner, placed in an autoclave, and heated to 383 K for 24 h. After reaction, the crystal was collected by filtration, washed with DMF (10 mL×3) and water (10 mL×3), and finally dried at 80 °C for 4 h.

Preparation of iron oxide

The magnetic particles were synthesized by the chemical coprecipitation method. $FeCl_3 \cdot 6H_2O$ (5.4 g) and $FeCl_2 \cdot 4H_2O$ (2.0 g) were dissolved in a 6.0 mol L^{-1} hydrochloric acid solution (25 mL), which was then sufficiently degassed with a nitrogen stream. After that, a 25 % (*v*/*v*) ammonium hydroxide solution (30 mL) was added to the solution with

vigorous stirring at 60 °C for 30 min under a nitrogen atmosphere. After cooling to ambient temperature, the resultant magnetic particles were attracted to the bottom by a magnet. The black products were washed several times sequentially with sufficient volumes of water and ethanol and then dried at 60 °C for 6 h.

Preparation of Fe_3O_4/IRMOF-3

For the synthesis of Fe_3O_4/IRMOF-3, 0.5 g R_3-BDC was dissolved in 40 mL DMF, and the mixture was poured into a 250 mL round-bottomed flask. Under magnetic stirring, Fe_3O_4 (70 mg) dissolved in 20 mL DMF was added and refluxed for a while at 90 °C. Next, 1.0 g $Zn(NO_3)_2 \cdot 6H_2O$ dissolved in 40 mL DMF were added to the above solution. After refluxing for 4 h, the product was collected by vacuum suction filtration, washed with DMF (10 mL×3) and water (10 mL×3), and finally dried at 80 °C for 4 h.

Sample extraction and preconcentration procedure

15 mg of Fe_3O_4/IRMOF-3 were added to 10 mL of sample solution containing the analyte ions and the pH of the solution was adjusted to 5 with 0.1 mol L^{-1} HNO_3 or 0.1 mol L^{-1} NaOH solutions. The mixed solution was then shaken at room temperature for 15 min to facilitate adsorption of Cu^{2+} onto the sorbent. Subsequently, the magnetic sorbent with adsorbed copper was separated from the mixture using a permanent magnet. The magnet was removed and 1 mL of 0.1 mol L^{-1} NaCl solution (pH=2)was added as eluent and stirred for 15 min. Finally, the magnet was used again to settle the magnetic sorbent, and the eluate was transferred into a test tube for subsequent ETAAS analysis.

Samples and sample pretreatment

The water samples were collected locally. The samples were filtered immediately after sampling, and stored at 4 °C. Before the experiment, 10 mL of the water samples were diluted to 100 mL with de-ionized water. Certified reference materials stream sediment (GBW07303a): 0.5000 g of stream sediment were mixed with 10 mL HCl and heated at 150 °C for 1 h. After preliminary decomposition, 5 mL HNO_3 and 3 mL $HClO_4$ were added and the mixtures were heated at 250 °C until the solution was nearly dried. After cooling, the residue was diluted to 50 mL with de-ionized water. Certified reference materials soil (GBW07405): 0.5000 g of soil is mixed with 10 mL HNO_3 and 5 mL $HClO_4$. After soaking for one night at room temperature, 1 mL H_2O_2 and 1 mL HCl were added and heated at 180 °C to dissolve the soil until the residues become milky. After cooling, 10 mL HNO_3 was added to make the solution clear and transparent. Finally, the content was diluted to 50 mL with de-ionized water.

Results and discussion

Characterization of the sorbent

FTIR spectrums of IRMOF-3 and Fe_3O_4/IRMOF-3 in the range of 4,000–400 cm^{-1} were recorded using the KBr pellet method (Fig. S1, Electronic Supplementary Material, ESM). As for IRMOF-3, two peaks appeared at 3,126 and 3,317 cm^{-1}, corresponding to the presence of the amino groups. The two sharp bands at 1,560 and 1,388 cm^{-1} correspond to the asymmetric and symmetric vibrations of carboxyl groups, respectively. The peak appearing at 1,232 cm^{-1} can be assigned to C–N vibrations. The FTIR spectrum of Fe_3O_4/IRMOF-3 is similar to that of IRMOF-3, except for a stronger peak at 575 cm^{-1}, which can be assigned to the stretching of Fe–O bond, indicating that Fe_3O_4 was successfully introduced into IRMOF-3.

Figure 1 shows X-ray diffraction patterns of IRMOF-3 and Fe_3O_4/IRMOF-3. The XRD pattern (Fig. 1a) of IRMOF-3 is very similar to that reported in the literature [32]. When combined with Fe_3O_4, the similar peak positions show that the structure of IRMOF-3 was preserved, although the peak intensities decreased. The decrease in the peak intensities after modification can be attributed to the decrease in the crystallinity. Meanwhile, the change in the peak intensities indicated the successful synthesis of magnetic IRMOF-3.

The hysteresis curves measured at T=293 K for Fe_3O_4 and Fe_3O_4/IRMOF-3 are compared in Fig. 2. Neither coercivity nor remanence was observed, suggesting that the two particles are superparamagnetic. The saturation magnetization value was measured to be 80.92 emu g^{-1} for Fe_3O_4 and 20.25 emu g^{-1} for Fe_3O_4/IRMOF-3. Compared with Fe_3O_4, the magnetic strength of Fe_3O_4/IRMOF-3 decreased due to the presence of IRMOF-3. However, it was sufficient for magnetic separation with common magnets.

To investigate the surface morphology of IRMOF-3 and Fe_3O_4/IRMOF-3, the samples were characterized by SEM (Fig. S2, ESM). IRMOF-3 (Fig. S2-a) is obtained as well-formed cubic crystals with a rather smooth surface. In comparison with IRMOF-3, the SEM image of Fe_3O_4/IRMOF-3 (Fig. S2-b) keeps the crystal morphology, and the surface of Fe_3O_4/IRMOF-3 tends to be rougher after immobilization by Fe_3O_4. When combined with Fe_3O_4, the size of crystals became obviously smaller. It may be that the addition of Fe_3O_4 restricted the growth of the crystals, or it may be due to the different synthesis methods used in the cases of IRMOF-3 and Fe_3O_4/IRMOF-3.

Thermogravimetric analysis (TGA) of IRMOF-3 and Fe_3O_4/IRMOF-3 in nitrogen was also investigated (Fig. S3, ESM). IRMOF-3 shows an initial weight loss of about 6 wt% below 350 °C, due to the release of the remaining DMF, and a second weight loss of ca. 48 wt% due to the decomposition of organic linkers of the framework between 350 and 550 °C. As

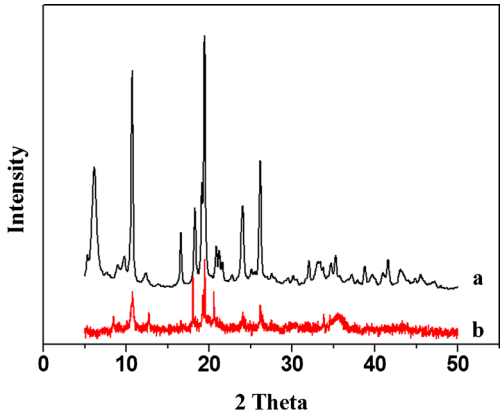

Fig. 1 XRD patterns of IRMOF-3(**a**) and Fe_3O_4/IRMOF-3 (**b**)

shown in Fig. S3-b, Fe_3O_4/IRMOF-3 has the same thermal behavior as IRMOF-3, indicating that the Fe_3O_4/IRMOF-3 is stable up to 350 °C. Furthermore, the remaining amount of Fe_3O_4/IRMOF-3 is larger than that of IRMOF-3, which due to the presence of Fe_3O_4 particles.

Optimization of instrument measurement conditions

Preliminary experiments indicated that the temperature program suggested by manufacturers could not be efficient for this method. As key parameters in the atomization process, the pyrolysis and the atomization temperatures were investigated in this work.

The optimal pyrolysis temperature needs to be high enough to cause the interfering components to volatilize completely. In addition, in order to avoid losing the analytes during pyrolysis, the pyrolysis temperature should be as low as possible. The pyrolysis temperature of the sample solutions containing 50 μg L^{-1} of copper ions was adjusted in the range of 500–900 °C (Fig. 3a). The absorbance increased as the temperature increased, and reached a maximum value at 800 °C. With temperatures higher than this, loss of analyte occurred. Therefore, a pyrolysis temperature of 800 °C was selected.

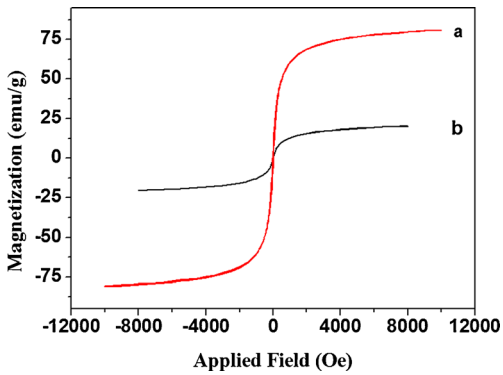

Fig. 2 VSM magnetization curves of Fe_3O_4 (**a**) and Fe_3O_4/IRMOF-3 (**b**)

The atomization temperature of the sample solutions containing 50 μg L^{-1} of copper ions was studied in the range of 1,700–2,200 °C (Fig. 3b). With the temperature rise, the absorbance increased, and remained unchanged at 2,000–2,200 °C. The lower atomization temperature is beneficial in terms of prolonging the service life of the graphite tube. Therefore, the best atomization temperature is 2,100 °C.

Optimization of the adsorption conditions

The pH of the solution is one of the most important parameters influencing the adsorption process of metal ions on the sorbent because of the protonation or deprotonation reaction for the sorbent and the hydrolysis reaction for the metal ions in the alkaline condition. Therefore, pH is the first parameter to be optimized. In this series of experiments, the solution pH was varied over the range of 2 to 7 with 0.1 mol L^{-1} HNO_3 or 0.1 mol L^{-1} NaOH solutions. As shown in Fig. 4, the adsorption efficiency increased with the increasing pH of the solution. Adsorption efficiency was calculated using the following equation:

$$\text{Adsorption efficiency}\% = \left((C_a - C_b)/C_a\right) \times 100$$

where C_a and C_b are initial and final concentrations of copper ions in the solution, respectively.

The change in adsorption characteristics with solution pH may be more clearly understood from the relevant equations (see supplementary material) [33], which depict the major characteristic reactions that can take place at the solid-solution interface of Fe_3O_4/IRMOF-3. With increasing solution pH, it can be reasonably speculated that the adsorption of Cu^{2+} can occur in three ways: (1) coordination between $-NH_2$ from Fe_3O_4/IRMOF-3 and Cu^{2+}; (2) electrostatic attraction between negative $-NH_2OH^-$ and positive Cu^{2+} (or $CuOH^+$); (3) an ion exchange process between $-m$FeOH and Cu^{2+}. When pH continues to increase, the precipitate of $Cu(OH)_2$ appears. Hence, the subsequent studies were carried out using a sample pH of 5.

Adsorption time is one of the main factors affecting the adsorption process. If the adsorption time is not sufficient, the sorbent could adsorb the metal ion incompletely. The effect of adsorption time on the adsorption efficiency of the solution of 1.0 μg L^{-1} Cu^{2+} in the range of 5–25 min was studied. As the adsorption time increased from 5 to 15 min, the adsorption efficiency for Cu^{2+} increased, and further prolonging of the adsorption time did not significantly increase the adsorption efficiency (Fig. S4, ESM). Thus, 15 min is the best adsorption time.

For solid phase extraction processes, a smaller amount of sorbent may result in incomplete adsorption, whereas a larger

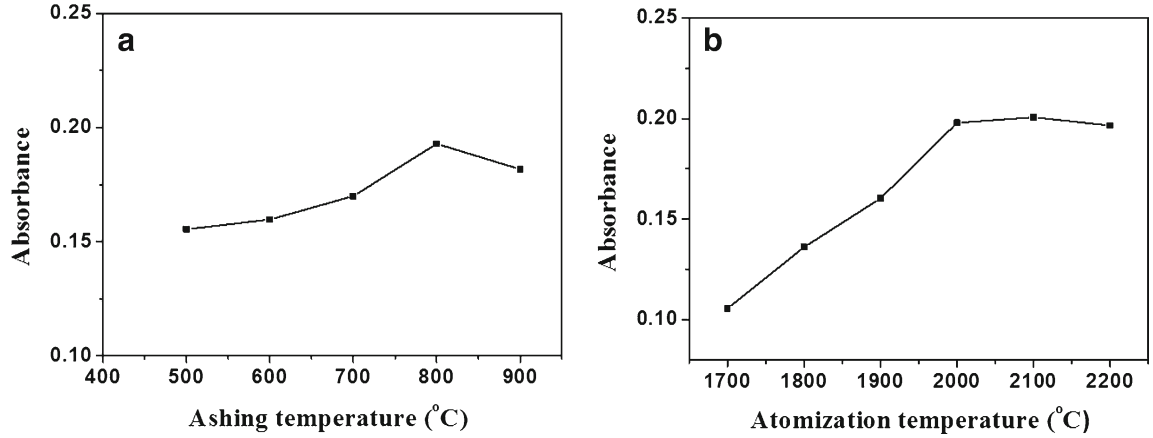

Fig. 3 Pyrolysis (**a**) and atomization temperature (**b**) curves for copper. Conditions: 50 μg L^{-1} Cu^{2+} solution, pH=5; instrument conditions: wavelength: 324.8 nm, lamp current: 6 mA, spectral bandpass: 0.2 nm, drying temperature: 90 °C, cleaning temperature: 2,200 °C, argon purge gas flow rate: 1,000 mL min^{-1}, determination mode: peak area

amount of sorbent increases the interference of the coexisting metal ions. Thus, the amount of sorbent is one of the most important parameters influencing the adsorption process of metal ions on the sorbent. In order to determine the optimal amount of sorbent, different amounts (5–20 mg) of the sorbent were added to the solution of 10 mL 1.0 μg L^{-1} Cu^{2+} to examine the effect on adsorption of Cu^{2+} ion on Fe_3O_4/IRMOF-3 (Fig. S5, ESM). The experimental results show that the adsorption efficiency increased with an increasing amount of absorbent due to the increase of the amount of adsorption surface area and the number of functional groups involved in adsorption. When the sorbent was above 15 mg, the adsorption efficiency increased slowly and reached equilibrium. Therefore, 15 mg of Fe_3O_4/IRMOF-3 was selected for use in further studies.

From the pH study, it was found that the adsorption of Cu^{2+} on Fe_3O_4/IRMOF-3 at lower solution pH was negligible. This suggested that desorption of Cu^{2+} on Fe_3O_4/IRMOF-3 was possible at lower solution pH. In this work, eluents (H_2SO_4, HCl, HNO_3, NaCl) were chosen as the desorption solvent. Results show that H_2SO_4, HCl and HNO_3 will decompose the structure of Fe_3O_4/IRMOF-3, but at different pH levels, NaCl increases recovery without any decomposition of Fe_3O_4/IRMOF-3 structure. Therefore, 0.1 mol L^{-1} of NaCl solutions with different pH (1, 2 and 3) and volumes were chosen for further study. Based on measurements, 1 mL of 0.1 mol L^{-1} NaCl solution (pH=2) was sufficient to elute the analyte, and was further employed throughout this work.

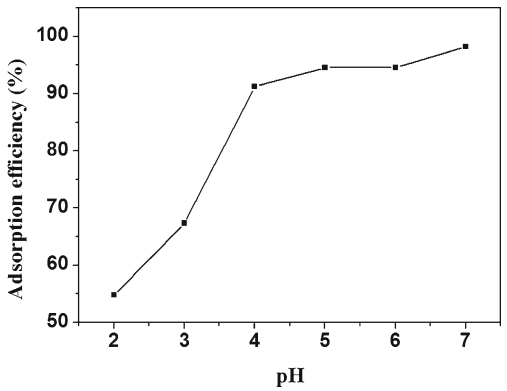

Fig. 4 Effect of sample solution pH on the sorption efficiency of Cu^{2+} on Fe_3O_4/IRMOF-3. Conditions: 10 mL 1.0 μg L^{-1} Cu^{2+} solution, extraction time: 15 min, amount of sorbent: 15 mg. Desorption conditions: 1 mL of 0.1 mol L^{-1} NaCl, pH=2, 15 min. Instrument conditions: as show in Fig. 3

Desorption time was evaluated in the range of 5–25 min. The experimental results indicated that a quantitative recovery of all analytes in 10 mL of sample solution was achieved when the stirring time was greater than 15 min for adsorption. Therefore, a desorption time of 15 min was used in subsequent experiments.

In the analysis of real samples, the maximum sample volume is an important factor in achieving a high enrichment factor. Under optimum conditions, the effect of sample volume on quantitative adsorption of Cu^{2+} was investigated in the range of 10–250 mL, and the total amount of Cu^{2+} was kept constant in 1.0 μg. Based on measurements, the recovery of Cu^{2+} was more than 95 % in the case of sample volumes up to 50 mL, and a decrease was observed with further increases in sample volume. With an elution volume of 1 mL, a theoretical enrichment factor of 50 was achieved by this method. However, for convenience, all the experiments were carried out with 10 mL of the aqueous phase.

Adsorption capacity is an important factor corresponding to the performance of the absorbent. In order to determine the adsorption capacity, 10 mg of Fe_3O_4/IRMOF-3 and 50 mL of 1 mg L^{-1} Cu^{2+} were equilibrated for 30 min. The maximum adsorption capacity has been found to be 2.4 mg g^{-1}. Under the same conditions, the adsorption capacity of Fe_3O_4 for

Table 1 Determination of Cu^{2+} in real water samples

Sample	Determined by present method (μg L^{-1})	Added (μg L^{-1})	Found (μg L^{-1})	Recovery (%)
Tap water	3.85±0.27	1.00	4.83±0.31	102.0
		5.00	8.78±0.37	100.6
Lake water	2.08±0.14	1.00	3.02±0.18	98.0
		5.00	6.98±0.33	101.8

Cu^{2+} was 0.36 mg g^{-1}. The results showed that the adsorption on copper was the synergistic effect of IRMOF-3 and Fe_3O_4.

The interferences

For demonstrating the selectivity of the procedure developed, the interference of alkali, alkaline earth and heavy metals, which are common elements in environmental samples, was investigated under the above optimized conditions. For this purpose, a solution of 1.0 μg L^{-1} Cu^{2+} containing the corresponding interfering ion alone was prepared, and an ion was considered to have interfered when its presence produced a variation of more than±5 %. The results showed that 300-fold concentrations of Cd^{2+}, Pb^{2+}, 200-fold concentrations of Cr^{2+}, Ag^{+}, 100-fold concentrations of Co^{2+}, Mn^{2+}, Sn^{2+}, 50-fold concentration of Ni^{2+}, Zn^{2+} have no influence on the signals of Cu^{2+}. The influence of some inorganic ions such as Na^{+}, K^{+}, Ca^{2+}, Mg^{2+}, Cl^{-}, NO_3^{-}, SO_4^{2-}, CO_3^{2-}, PO_4^{3-} could exist at concentrations of at least 10,000-fold. The above results indicated that the method developed is suitable for the analysis of Cu^{2+} in real samples and no further treatment or masking reagents are needed.

Performance and analytical applications

The analysis of a series of solutions containing 0.1, 0.5, 1.0, 5.0, and 10.0 μg L^{-1} Cu^{2+}, respectively, gave a calibration function of A=0.0768C (μg L^{-1})+0.0188, with a correlation coefficient of 0.9996. According to the IUPAC definition, the instrumental detection limit (3σ) for Cu^{2+} was 0.073 μg L^{-1}. Relative standard deviation of the procedure determined by 10 replicates of samples containing 0.1 μg L^{-1} Cu^{2+} was calculated to be 0.4 %. Determination of Cu^{2+} using the magnetic solid-phase extraction procedure developed was compared with the other procedures reported in the literature [34–37] (Table S1, ESM). The results indicated that the adsorption capacity, limit of detection, and enrichment factor of the method developed is better than those of the other methods used for the separation and preconcentration of copper. Other advantages of this method are: (1) Magnetic IRMOF-3 composite could be easily produced with a larger surface area and highly active surface sites. (2) The presence of the free amine functionality in the linker enhances the selectivity of the new solid phase towards copper. (3) The separation of copper-adsorbed magnetic adsorbent from the solution can easily be achieved via an external magnetic field. Therefore, satisfactory results can be achieved using lower volumes of sorbent. Regeneration is one of the key factors in evaluating the performance of the sorbent. It was found that the prepared Fe_3O_4/IRMOF-3 composite was relatively stable up to at least 10 adsorption-elution cycles without any obvious decrease in recovery. In order to demonstrate the performance of the method, tap water from laboratory and natural water from Slender West Lake were analyzed for the presence of copper. The results are given in Table 1 and indicate that the recoveries were reasonable for trace analysis, in a range of 98.0–102.0 %. To further establish the validity of the procedure, the method was applied to the determination of the content of Cu^{2+} in standard reference materials: GBW07303a (stream sediment) and GBW07405 (soil). The experimental results demonstrated good agreement with the certified values (Table 2). In conclusion, the analytical procedure is accurate and precise for copper determination in real samples.

Conclusion

In this research, a novel superparamagnetic Fe_3O_4/IRMOF-3 sorbent was successfully synthesized and applied for separation and preconcentration of heavy metal ions before determination by ETAAS. Compared with traditional SPE methods, this SPE method has the following merits: (a) the abundant amine groups in IRMOF-3 demonstrate high adsorption capacity and extraction efficiency for the target analyte. (b) superparamagnetic Fe_3O_4/IRMOF-3 sorbents can be easily collected and eluted with the help of a magnet. This research has not only developed a rapid and convenient MSPE method for the extraction of heavy metal ions from complicated samples, but has also extended the scope of applications of metal-organic framework.

Table 2 Validation of the method for the determination of Cu^{2+} in certified reference materials

Sample	Certified value (μg g^{-1})	Found value (μg g^{-1})	RSD(%)
GBW07405	166±9	162±6	3.7
GBW07303a	202±7	205±5	2.4

Acknowledgments This work was supported by the National Natural Science Foundation of China (21205103, 21275124), Jiangsu Provincial Nature Foundation of China (BK2012258), and is a project funded by the Priority Academic Program Development of Jiangsu Higher Education Institutions.

References

1. Shakerian F, Dadfarnia S, Haji Shabani AM, Shiralian Esfahani G (2013) Preconcentration and determination of lead(II) by microextraction based on suspended cadion covered zirconia nanoparticles in a surfactant media. Microchim Acta 180:1225
2. Zeng SL, Gan N, Weideman-Mera R, Cao YT, Li TH, Sang WG (2013) Enrichment of polychlorinated biphenyl 28 from aqueous solutions using Fe_3O_4 grafted graphene oxide. Chem Eng J 218:108
3. Heidari H, Razmi H (2012) Multi-response optimization of magnetic solid phase extraction based on carbon coated Fe_3O_4 nanoparticles using desirability function approach for the determination of the organophosphorus pesticides in aquatic samples by HPLC-UV. Talanta 99:13
4. Han Q, Wang ZH, Xia JF, Chen S, Zhang XQ, Ding MY (2012) Facile and tunable fabrication of Fe_3O_4/graphene oxide nanocomposites and their application in the magnetic solid-phase extraction of polycyclic aromatic hydrocarbons from environmental water samples. Talanta 101:388
5. Zhang XL, Niu HY, Pan YY, Shi YL, Cai YQ (2010) Chitosan-coated octadecyl-functionalized magnetite nanoparticles: preparation and application in extraction of trace pollutants from environmental water samples. Anal Chem 82:2363
6. Sun L, Sun X, Du XB, Yue YS, Chen LG, Xu HY, Zeng QL, Wang H, Ding L (2010) Determination of sulfonamides in soil samples based on alumina-coated magnetite nanoparticles as adsorbents. Anal Chim Acta 665:185
7. Wang Q, Huang LJ, Yu PF, Wang JC, Shen S (2013) Magnetic solid-phase extraction and determination of puerarin in rat plasma using C18-functionalized magnetic silica nanoparticles by high performance liquid chromatography. J Chromatogr B 912:33
8. Zhou YY, Yan XP, Kim KN, Wang SW, Liu MG (2006) Exploration of coordination polymer as sorbent for flow injection solid-phase extraction on-line coupled with high-performance liquid chromatography for determination of polycyclic aromatic hydrocarbons in environmental materials. J Chromatogr A 1116:172
9. Cui XY, Gu ZY, Jiang DQ, Li Y, Wang HF, Yan XP (2009) In situ hydrothermal growth of metal-organic framework 199 films on stainless steel fibers for solid-phase microextraction of gaseous benzene homologues. Anal Chem 81:9771
10. Yu LQ, Yan XP (2013) Covalent bonding of zeolitic imidazolate framework-90 to functionalized silica fibers for solid-phase microextraction. Chem Commun 49:2142
11. Chang N, Gu ZY, Wang HF, Yan XP (2011) Metal-organic-framework-based tandem molecular sieves as a dual platform for selective microextraction and high-resolution gas chromatographic separation of n-alkanes in complex matrixes. Anal Chem 83:7094
12. Gu ZY, Wang G, Yan XP (2010) MOF-5 metal-organic framework as sorbent for in-field sampling and preconcentration in combination with thermal desorption GC/MS for determination of atmospheric formaldehyde. Anal Chem 82:1365
13. Gu ZY, Yan XP (2010) Metal-organic framework MIL-101 for high-resolution gas-chromatographic separation of xylene isomers and ethylbenzene. Angew Chem Int Ed 49:1477
14. Gu ZY, Jiang JQ, Yan XP (2011) Fabrication of isoreticular metal–organic framework coated capillary columns for high-resolution gas chromatographic separation of persistent organic pollutants. Anal Chem 83:5093
15. Yang CX, Chen YJ, Wang HF, Yan XP (2011) High-performance separation of fullerenes on metal-organic framework MIL-101(Cr). Chem Eur J 17:11734
16. Yang CX, Yan XP (2011) Metal–organic framework MIL-101(Cr) for high-performance liquid chromatographic separation of substituted aromatics. Anal Chem 83:7144
17. Gu ZY, Yang CX, Chang N, Yan XP (2012) Metal organic frameworks for analytical chemistry: from sample collection to chromatographic separation. Acc Chem Res 45(5):734
18. Li LM, Wang HF, Yan XP (2012) Metal-organic framework ZIF-8 nanocrystals as pseudostationary phase for capillary electrokinetic chromatography. Electrophoresis 33:2896
19. Liu SS, Yang CX, Wang SW, Yan XP (2012) Metal–organic frameworks for reverse-phase high-performance liquid chromatography. Analyst 137:816
20. Yang CX, Liu SS, Wang HF, Wang SW, Yan XP (2012) High-performance liquid chromatographic separation of position isomers using metal–organic framework MIL-53(Al) as the stationary phase. Analyst 137:133
21. Fu YY, Yang CX, Yan XP (2013) Metal-organic framework MIL-100(Fe) as the stationary phase for both normal-phase and reverse-phase high performance liquid chromatography. J Chromatogr A 1274:137
22. Chang N, Gu ZY, Yan XP (2010) Zeolitic imidazolate framework-8 nanocrystal coated capillary for molecular sieving of branched alkanes from linear alkanes along with high-resolution chromatographic separation of linear alkanes. J Am Chem Soc 132:13645
23. Chang N, Yan XP (2012) Exploring reverse shape selectivity and molecular sieving effect of metal-organic framework UIO-66 coated capillary column for gas chromatographic separation. J Chromatogr A 1257:116
24. Ni Z, Jerrell JP, Cadwallader KR, Masel RI (2007) Metal-organic frameworks as adsorbents for trapping and preconcentration of organic phosphonates. Anal Chem 79:1290
25. Bagheri A, Taghizadeh M, Behbahani M, Asgharinezhad AA, Salarian M, Dehghani A, Ebrahimzadeh H, Amini MM (2012) Synthesis and characterization of magnetic metal-organic framework (MOF) as a novel sorbent, and its optimization by experimental design methodology for determination of palladium in environmental samples. Talanta 99:132
26. Sohrabi MR, Matbouie Z, Asgharinezhad AK, Dehghani A (2013) Solid phase extraction of Cd(II) and Pb(II) using a magnetic metal-organic framework, and their determination by FAAS. Microchim Acta 180:589
27. Taghizadeh M, Asgharinezhad AK, Pooladi M, Barzin M, Abbaszadeh A, Tadjarodi A (2013) A novel magnetic metal organic framework nanocomposite for extraction and preconcentration of heavy metal ions, and its optimization via experimental design methodology. Microchim Acta 180:1073
28. Eddaoudi M, Kim J, Rosi N, Vodak D, Wachter J, O'Keeffe M, Yaghi OM (2002) Systematic design of pore size and functionality in isoreticular MOFs and their application in methane storage. Science 295:469
29. Morris W, Taylor RE, Dybowski C, Yaghi OM, Garcia-Garibay MA (2011) Framework mobility in the metal-organic framework crystal IRMOF-3: evidence for aromatic ring and amine rotation. J Mol Struct 1004:94
30. Ali SA, Al Hamouz OCS, Hassan NM (2013) Novel cross-linked polymers having pH-responsive amino acid residues for the removal of Cu^{2+} from aqueous solution at low concentrations. J Hazard Mater 248–249:47
31. Llabresi Xamena FX, Cirujano FG, Corma A (2012) An unexpected bifunctional acid base catalysis in IRMOF-3 for knoevenagel condensation reactions. Microporous Mesoporous Mater 157:112

32. Zhang X, Xamena FX L i, Corma A (2009) Gold(III)-metal organic framework bridges the gap between homogeneous and heterogeneous gold catalysts. J Catal 265:155
33. Xin XD, Wei Q, Yang J, Yan LG, Feng R, Chen GD, Du B, Li H (2012) Highly efficient removal of heavy metal ions by amine-functionalized mesoporous Fe_3O_4 nanoparticles. Chem Eng J 184:132
34. Yu HM, Song H, Chen ML (2011) Dithizone immobilized silica gel on-line preconcentration of trace copper with detection by flame atomic absorption spectrometry. Talanta 85:625
35. Chamjangali MA, Bagherian G, Mokhlesian A, Bahramian B (2011) Synthesis and application of chloromethylated polystyrene modified with 1-phenyl-1,2-propanedione-2-oxime thiosemicarbazone (PPDOT) as a new sorbent for the on-line preconcentration and determination of copper in water, soil, and food samples by FAAS. J Hazard Mater 192:1641
36. Escudero LA, Cerutti S, Olsina RA, Salonia JA, Gasquez JA (2010) Factorial design optimization of experimental variables in the on-line separation/preconcentration of copper in water samples using solid phase extraction and ICP-OES determination. J Hazard Mater 183: 218
37. Cui C, He M, Hu B (2011) Membrane solid phase microextraction with alumina hollow fiber on line coupled with ICP-OES for the determination of trace copper, manganese and nickel in environmental water samples. J Hazard Mater 187:379